Femtosecond fiber laser at 780 nm for two-photon autofluorescence imaging

Wan Yang (杨 琬)[1], Danlei Wu (吴丹磊)[1,2], Runlong Wu (吴润龙)[1], Guanyu Liu (刘关玉)[1], Bingying Chen (陈冰影)[1], Lishuang Feng (冯丽爽)[2], Zhigang Zhang (张志刚)[1], and Aimin Wang (王爱民)[1,*]

[1]*State Key Laboratory of Advanced Optical Communication System and Networks, School of Electronics Engineering and Computer Science, Peking University, Beijing 100871, China*

[2]*Key Laboratory of Precision Opto-Mechatronics Technology, Ministry of Education, School of Instrumentation Science & Optoelectronics Engineering, Beihang University, Beijing 100191, China*

**Corresponding author: wangaimin@pku.edu.cn*

Received November 30, 2018; accepted April 12, 2019; posted online July 1, 2019

We present an Er-doped fiber (Er:fiber)-based femtosecond laser at 780 nm with 256 MHz repetition rate, 191 fs pulse duration, and over 1 W average power. Apart from the careful third-order dispersion management, we introduce moderate self-phase modulation to broaden the output spectrum of the Er:fiber amplifier and achieve 193 fs pulse duration and 2.43 W average power. Over 40% frequency doubling efficiency is obtained by a periodically poled lithium niobate crystal. Delivering through a hollow-core photonic bandgap fiber, this robust laser becomes an ideal and convenient light source for two-photon autofluorescence imaging.

OCIS codes: 140.7090, 140.3500, 140.3515.
doi: 10.3788/COL201917.071405.

Femtosecond lasers at 780 nm are vital sources for abundant applications, especially in two-photon fluorescence microscopy (TPFM)[1]. Some intrinsic molecules can be excited at 700–800 nm for two-photon autofluorescence microscopy (TPAM), such as nicotinamide adenine dinucleotide (phosphate) [NAD(P)H], flavin adenine dinucleotide (FAD), and keratin, which can be used to evaluate the state of metabolism or cell morphology. Therefore, it can be a potentially noninvasive approach to diagnosis and therapeutic monitoring[2–4]. Thus, the robust and low-cost femtosecond laser at 780 nm is an important light source for TPFM.

High repetition-rate laser pulses have attracted much attention for the low photobleaching rate[5] with a great increase of imaging speed and throughput. In our work, the repetition rate was chosen to be 256 MHz, which is a little lower than 333 MHz on account of the typical lifetime for most fluorophores (~3 ns)[6]. The pulse energy requirement of the femtosecond pulses for a basic-type TPFM is about 1–2 nJ with the average power around 100 mW, which is mainly decided by two-photon threshold and the power handling of the samples. However, higher power up to the Watt level is always preferred for more powerful microscopy combined with other technologies. For example, the newly developed miniature TPFM makes it possible to build a miniature TPFM system with multi-probes for the study of different targets simultaneously[7]; moreover, to obtain faster imaging speed, the Bessel beam could be used to do volumetric imaging with much higher laser power requirements[8].

Frequency doubling of femtosecond Er-doped fiber (Er:fiber) lasers[9–11] to obtain 780-800 nm pulses is more attractive than for Ti:sapphire lasers in terms of cost, compactness, and portability. There have been a lot of reports on the generation of femtosecond pulses at the 800 nm wavelength band based on Er:fiber lasers, but none of them showed high repetition rate (over 100 MHz), short pulse duration (~200 fs), and high average power (over 1 W) simultaneously. Reference [9] reported a miniature fiber-optic multi-photon microscopy (MPM) system with 80 mW pulses at 786 nm. However, strong side lobes degrade the pulse quality.

In this Letter, by combining fiber chirped pulse amplification (FCPA)[12] and self-phase modulation, we demonstrated a fiber laser of 256 MHz repetition rate, 191 fs pulse duration, and 1 W average power at 780 nm. A hollow-core photonic bandgap fiber (HC-PBF) was used to deliver the femtosecond pulses into the home-built two-photon microscope, and the autofluorescence imaging of rabbit intestine tissue and human skin was presented with this laser.

The system consists of an Er:fiber femtosecond laser, a fiber stretcher, a two-stage amplifier, a transmission grating pair compressor, and a frequency doubling system, shown in Fig. 1. The laser is a home-made dispersion-managed Er:fiber laser mode-locked by nonlinear polarization rotation (NPR)[13]. It generates sub-60-fs Fourier-transform-limited optical pulses with 40 mW average power and 256 MHz repetition rate. The short pulses are stretched by a 6.6-m-long dispersion compensating fiber (DCF) which has positive second-order dispersion and negative third-order dispersion (TOD) at 1560 nm, and the splicing loss is 1.46 dB. The stretched pulses are then pre-amplified up to 0.8 nJ by a 3.1-m-long single-mode Er:fiber (Er40-4/125, Liekki) and sent to the main amplifier, which is a 3.0-m-long double cladding Er/Yb co-doped

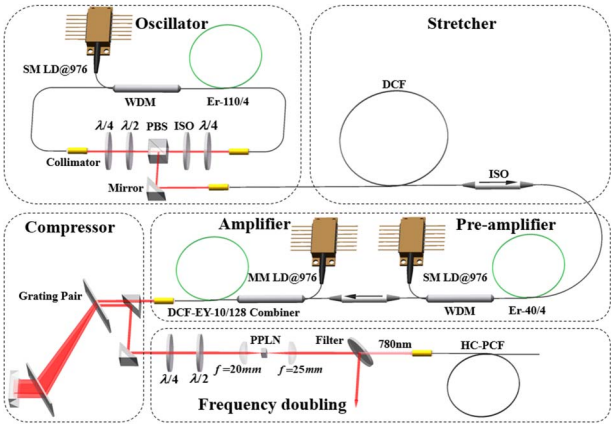

Fig. 1. Schematic diagram of the laser system. PBS, polarization beam splitter; SM LD, single-mode laser diode; MM LD, multimode laser diode; WDM, wavelength division multiplexer; ISO, isolator.

fiber (DCF-EY-10/128, CorActive), pumped by 16 W laser diodes at 976 nm. The two splice points of the main gain fiber were specially treated for dust prevention and heat dissipation[10].

It is important to match the dispersion at least to the third order to achieve pulses of about 100 fs. The dispersion at 1560 nm for all system components is listed in the Table 1. Obviously, the grating with groove density of 600 l/mm ($\beta_3/\beta_2 = -3.89$ fs) matches better with the DCF ($\beta_3/\beta_2 = -5.78$ fs) than the 966 l/mm ($\beta_3/\beta_2 = -9.24$ fs). Therefore, we chose 600 l/mm at the expense of longer grating distance.

The compressed pulses are frequency doubled by a 1-mm-long periodically poled lithium niobate (PPLN) crystal. The crystal is mounted on a copper holder for natural cooling. Two waveplates are utilized to rotate the polarization, ensuring maximum frequency doubling efficiency. A bandpass filter is used to remove the unwanted pulses from the frequency doubled pulses. Finally, the pulses at 780 nm are imported into a 1.5-m-long HC-PBF with negligible bending loss and nonlinearity[14]. No prechirp is needed because the dispersion of the HC-PBF at 780 nm is 14 ps/(nm·km).

The final output power after two-stage amplification is 3.6 W, and the optimized pulses are compressed to 193 fs. The average power of the compressed pulses is 2.43 W with the compression efficiency of 67.5%. To achieve this pulse duration, the DCF length was optimized.

Table 1. Dispersion of the FCPA System

Component	Other Fibers	Fiber Stretcher	Grating Compressor	
Type	SMF-28	DCF	966 l/mm	600 l/mm
β_2 (fs^2/mm)	−22	170	−14871	−3107
β_3 (fs^3/mm)	127	−983	137369	12085
β_3/β_2 (fs)	−5.77	−5.78	−9.24	−3.89

When the DCF length was 13.4 m, the spectrum bandwidth of the pulses was reduced from 52.6 nm of the seed pulses to 12.9 nm after two-stage amplification, so the compressed pulses were over 200 fs accordingly. To cope with the spectrum narrowing, we introduced a certain amount of nonlinear phase shift by a shorter stretched pulse in the DCF. The nonlinear phase shift is defined by

$$B = \frac{2\pi}{\lambda}\int_0^L n_2 I(z)\,\mathrm{d}z, \tag{1}$$

where λ is the central wavelength of the input pulses, I is the peak power of the input pulses, and n_2 is the nonlinear index of the material.

The nonlinear phase shift and the residual TOD as functions of the DCF length are shown in Fig. 2(a). Figure 2(b) shows the pulse spectra and the pulse duration as the DCF length is cut short from 13.4 to 4.5 m with 16 W pump power at 976 nm. Indeed, the pulse spectrum is broadened from 12.9 to 23.8 nm. However, side lobes appear with the shortest DCF, which can be reckoned as the contribution of excessive nonlinear phase shift. There should be a compromise between the spectrum width and the pulse profile.

By investigating the DCF length, we found that when the DCF length was 6.6 m, the pulse spectrum was about 20 nm, and the pulse duration was 193 fs with small side lobes, which is about 1.2 times the Fourier-transform-limited pulse duration.

Using the above optimized output pulses, we continued the frequency doubling and show the results in Fig. 3. Figure 3(a) shows the RF spectrum of the oscillator. Figure 3(b) shows the output average power of pulses at 780 nm as a function of the pump power. The maximum average power was 1.01 W, giving a frequency doubling efficiency of 41.6%. Figures 3(c) and 3(d) indicate the spectrum bandwidth of 5.9 nm and the pulse duration of 191 fs. Figure 4 shows the optical spectra of the frequency doubling under different DCF lengths with 16 W pump

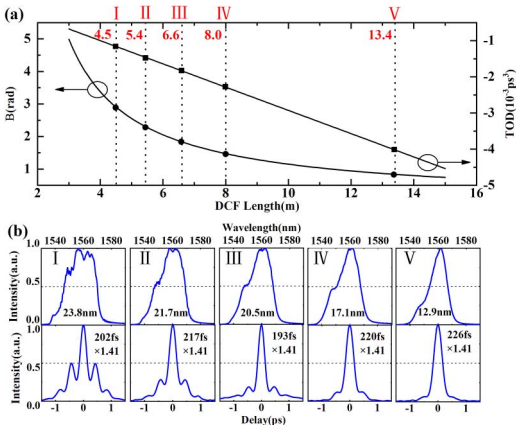

Fig. 2. Results of the Er:fiber laser. (a) Calculated nonlinear phase shift and residual TOD in the FCPA system, (b) spectra and intensity autocorrelation traces under different DCF lengths.

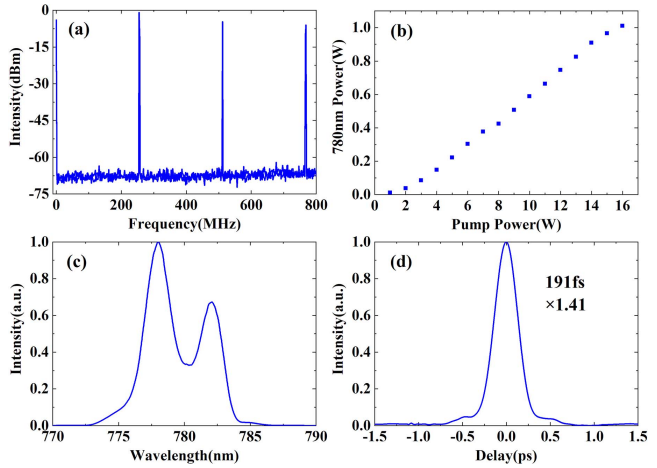

Fig. 3. Experimental results of the frequency doubling. (a) RF spectrum of the oscillator, (b) output average power, (c) optical spectrum, (d) intensity autocorrelation trace of the frequency doubled pulse.

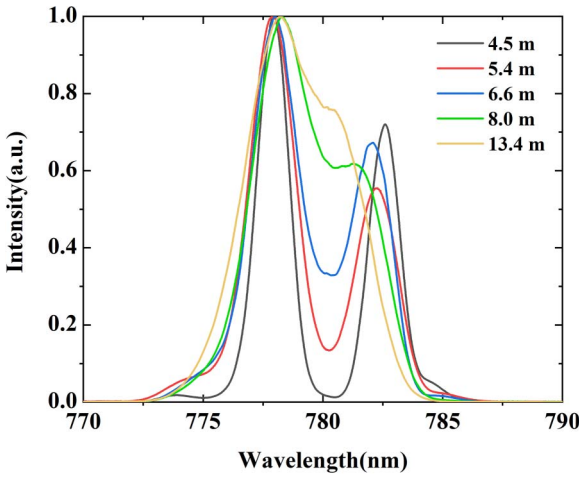

Fig. 4. Optical spectra of frequency doubling under different DCF lengths.

power for the Er:fiber laser. The shorter the DCF is, the deeper the gap in the spectrum would be. The asymmetry of the pulse spectrum profile at 780 nm is caused by the accumulated nonlinear phase shift in fundamental pulses at 1560 nm.

The output pulses from the HC-PBF were launched into a home-built two-photon microscope to image the rabbit intestine tissue and human skin. The average powers of the samples were 85 and 40 mW, respectively. Figure 5(a) displays the TPAM image of the rabbit intestinal epithelium *ex vivo* with a bandpass filter (40 nm at 460 nm) for autofluorescence signals collection. There are strong fluorescence signals from the NAD(P)H in the mitochondria and cytosol. Figure 5(b) displays the TPAM images of the human skin *in vivo* at depths from 0 to 30 μm below the surface. A 450 nm longpass filter was used to collect autofluorescence signals from NAD(P)H, FAD, keratin, and so on. The morphology features at different depths could be clearly seen.

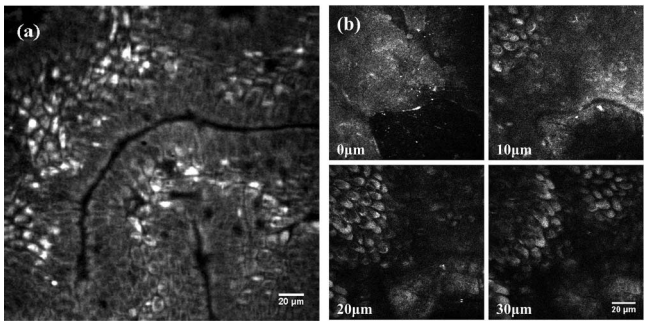

Fig. 5. (a) Experimental result of TPAM imaging of the rabbit intestine tissue *ex vivo*. Image size: 248 μm. Scale bar: 20 μm. (b) Experimental result of TPAM imaging of the human skin *in vivo* at different depths. Image size: 130 μm. Scale bar: 20 μm.

We have demonstrated an FCPA laser at 780 nm, which generates 256 MHz, 191 fs, and 1.01 W average power pulses. The pulse energy is 3.95 nJ with 20.68 kW peak power. Through careful TOD and nonlinearity management, high power and good quality pulses at 780 nm are obtained. Two-photon autofluorescence imaging of the rabbit intestine tissue and human skin with this laser was performed, and the result confirms the great potential of the laser to be used for diagnosis and therapeutic monitoring without the use of extrinsic labels. The integrated fiber laser source with a miniature TPFM system will be investigated in our future study.

This work was supported in part by the National Natural Science Foundation of China (Nos. 61475008 and 31327901).

References

1. W. Denk, J. H. Strickler, and W. W. Webb, Science **248**, 73 (1990).
2. D. Pouli, M. Balu, C. A. Alonzo, Z. Liu, K. P. Quinn, F. Rius-Diaz, R. M. Harris, K. M. Kelly, B. J. Tromberg, and I. Georgakoudi, Sci. Transl. Med. **8**, 367ral69 (2016).
3. W. R. Zipfel, R. M. Williams, R. Christie, A. Y. Nikitin, B. T. Hyman, and W. W. Webb, Proc. Natl. Acad. Sci. India. **100**, 7075 (2003).
4. M. Balu, K. M. Kelly, C. B. Zachary, R. M. Harris, T. B. Krasieva, K. Konig, A. J. Durkin, and B. J. Tromberg, Cancer Res. **74**, 2688 (2014).
5. N. Ji, J. C. Magee, and E. Betzig, Nat. Methods **5**, 197 (2008).
6. M. Y. Berezin and S. Achilefu, Chem. Rev. **110**, 2641 (2010).
7. W. Zong, R. Wu, M. Li, Y. Hu, Y. Li, J. Li, H. Rong, H. Wu, Y. Xu, Y. Lu, H. Jia, M. Fan, Z. Zhou, Y. Zhang, A. Wang, L. Chen, and H. Cheng, Nat. Methods **14**, 713 (2017).
8. B. Chen, H. Rong, X. Huang, R. Wu, D. Wu, Y. Li, L. Feng, Z. Zhang, L. Chen, and A. Wang, Opt. Express **25**, 22704 (2017).
9. L. Huang, A. K. Mills, Y. Zhao, D. J. Jones, and S. Tang, Biomed. Opt. Express **7**, 1948 (2016).
10. Z. Liu, W. Zong, Y. Liu, L. Zuo, C. Wen, T. Jiang, J. Zhang, Y. Ma, Z. Zhang, L. Chen, and A. Wang, in *Conference on Lasers and Electro-Optics (CLEO)* (2015), paper AM1J.6.
11. P. Elahi, H. Kalaycıoğlu, H. Li, Ö. Akcaalan, and F. Ö. Ilday, Opt. Cummun. **403**, 381 (2017).
12. D. Strickland and G. Mourou, Opt. Commun. **55**, 447 (1985).
13. D. Ma, Y. Cai, C. Zhou, W. Zong, L. Chen, and Z. Zhang, Opt. Lett. **35**, 2858 (2010).
14. W. Göbel, A. Nimmerjahn, and F. Helmchen, Opt. Lett. **29**, 1285 (2004).